Structure Determination and Luminescent Property Studies of the Single Crystal Na$_3$Sm(BO$_3$)$_2$

Dan Zhao [1],*, Fa-Xue Ma [1], Cong-Kui Nie [1], Jian Wang [2],*, Lei Zhang [1] and Yunchang Fan [1]

[1]   College of Chemistry and Chemical Engineering, Henan Polytechnic University, Jiaozuo 454003, China;
      mafaxue2017@163.com (F.-X.M.); niecongkui2017@163.com (C.-K.N.);
      leizh2008@163.com (L.Z.); fanyunchang@hpu.edu.cn (Y.F.)
[2]   College of Physics and Electronic Information, Henan Polytechnic University, Jiaozuo 454003, China
*   Correspondence: iamzd1996@163.com (D.Z.); jianwang@hpu.edu.cn (J.W.)

Abstract: Sodium samarium borate Na$_3$Sm(BO$_3$)$_2$, was prepared by a flux method and structurally characterized by single-crystal structure analysis for the first time. The results show that it crystallizes in the monoclinic system $P2_1/n$, with a = 6.5667(3) Å, b = 8.7675(4) Å, c = 10.1850(5), β = 90.86°, V = 586.32(5) Å^3 and Z = 4. The structure contains NaO$_7$, NaO$_6$, NaO$_5$, SmO$_8$, and BO$_3$ units, which are interconnected via corner- or edge-sharing O atoms into a three-dimensional structure. The excitation spectra, emission spectra, decay time, and Commission International de l'Éclairage (CIE) chromaticity index of Na$_3$Sm(BO$_3$)$_2$ were studied. Under near light excitation (406 nm), the powdered Na$_3$Sm(BO$_3$)$_2$ shows the orange-red emission, which originates from the $^4G_{5/2} \rightarrow {}^6H_{9/2}$ and $^4G_{5/2} \rightarrow {}^6H_{7/2}$ transformation of Sm^{3+} ion.

Keywords: borate compounds; flux method; crystal structure; luminescence

1. Introduction

In recent years, developing new luminescent materials has become a hot topic for new lighting and display technology such as phosphor-converted white light emitting diodes (LED) because of their excellent advantages of eco-friendliness, high efficiency, high power efficiency, long lifetime, and low cost [1–3]. The most commercially utilized kind of white LED is the combination of a blue LED chip with a yellow phosphor (Y$_3$Al$_5$O$_{12}$: Ce^{3+}), which blends the blue light from the chip and yellow light from the phosphor resulting in white light. However, this kind of white LED has the poor color rendering index and high Correlated Color Temperature (CCT) for the lack of red component. Another way is to directly use a near-ultraviolet (NUV) LED to excite red, green, and blue (RGB) multiphase phosphors to create warm-white light, which results in a great interest in searching for novel phosphors for white LEDs. The crystal matrix of host materials is one of the most important roles to determine the performance of phosphors. In recent years, a large amount of research work has been devoted to explore new phosphors in various host materials with high performance, good stability, and easily preparation [4,5].

Among various host materials, rare earth borates have been paid intense attention for a wide range of applications due to their significant advantages, such as a low sintering temperature, low cost, broad band gap, high luminous efficiency, and high chemical stability [6,7]. The boron atoms can coordinate to three and four oxygen atoms forming a BO$_3$ triangle and a BO$_4$ tetrahedron, respectively, and these units can further polymerize to complicated B$_x$O$_y$ architectures. Meanwhile, the rare earth ions within these borates possess a unique optical behavior and have paved the way for the development of optical phosphors. For these compounds, the electronic transitions originate from the partially filled 4f energy shell of rare earth ions, which are not influenced by the 5s and 5p electrons. These transitions lead to

narrow and intense emission bands, which are useful sources of individual colors in multicolor light emitting devices.

The crystal structure of sodium rare-earth borates $Na_3Ln(BO_3)_2$ (Ln = rare-earth metals) was first reported by Mascetti et al. for La and Nd species through single-crystal X-ray diffraction (SC-XRD), revealing the monoclinic space group $P2_1/c$ of this family [8]. Later on, the structure of three isotype compounds $Na_3Ln(BO_3)_2$ (Ln = Pr, Sm Eu) were studied by Wang et al., through powder XRD [9]. However, no single crystal data and luminescent properties were given for the ternary compound $Na_3Sm(BO_3)_2$ until now. We deem that single crystals of $Na_3Sm(BO_3)_2$ can be obtained by using a facile high temperature flux method, which is thought to be an effective and powerful tool in solid-state chemistry. In this method, the reactant materials are completely dissolved in molten salt to obtain a uniform liquid, and a single crystal with large size can then be obtained by limiting the number of nuclei formed during cooling. Up to now, many mixed-metal oxides, sulfides, and complex intermetallics have been successfully obtained using this method [10–13]. We think the Na_2O-B_2O_3 system can be used as a good flux for the low melting point (700~900 °C) and powerful dissolving capacity for many oxides, including refractory rare-earth oxides. Moreover, Na_2O-B_2O_3 mixed salt can easily be removed by washing with water after the reaction. Herein, we report the powder synthesis, single crystal preparation, and luminescent properties of $Na_3Sm(BO_3)_2$.

2. Experimental Section

2.1. Material and Methods

All of the chemicals Na_2CO_3 ($\geq$99.0%, Sinopharm Chemical Reagent Co., Ltd, Shanghai, China), Sm_2O_3 ($\geq$99.9%, Sinopharm Chemical Reagent Co.,Ltd, Shanghai, China) and H_3BO_3 ($\geq$99.0%, Sinopharm Chemical Reagent Co., Ltd, Shanghai, China) were used without further purification. X-ray powder diffraction (XRD) patterns were collected on a Rigaku DMax-2500 diffractometer (Rigaku Corporation, Tokyo, Japan) by using graphite-monochromated Cu Kα radiation in the angular range $2\theta = 5-75°$ with a step size of $0.02°$. TGA studies were all carried out with NETZSCH STA 449C instruments (NETZSCH-Gerätebau GmbH, Selb, Germany). The sample and reference (Al_2O_3) were enclosed in a platinum crucible and heated at a rate of 15 °C·min^{-1} from room temperature to 1000 °C under a nitrogen atmosphere. Photoluminescence (PL) spectra and the lifetime test were carried out using an FLS920 Edinburgh Analytical Instrument (Edinburgh Instruments Company, Edinburgh, Britain) apparatus. A standard Xe900 continuous-wave xenon lamp (450 W) was used as the excitation source for steady-state measurements (stimulation slit width: 2.0 nm, emission slit width: 2.0 nm). The PL excitation and emission spectra was recorded within 350–450 nm and 475–750 nm, respectively, with a step width of 1 nm and an integration time of 0.2 s. A standard microsecond flash lamp μF920H was used for excitation in lifetime measurements using the time-correlated single-photon counting (TCSPC) technique. The flash lamp operated at a pulse frequency of 2000 Hz with a pulse width of 2 μs. The decay was measured with a range of 10 μs, and counts at the maximum were 2000.

2.2. Synthetic Procedures

Powder sample of $Na_3Sm(BO_3)_2$ can be obtained in quantitative yield by the solid-state reaction of a mixture of Na_2CO_3 (2.000 g, 18.87 mmol), Sm_2O_3 (2.193 g, 6.289 mmol), and H_3BO_3 (1.555 g, 25.16 mmol) in a molar ratio of 3:1:4, which is similar to Wang's method [9]. The mixture was ground with an agate mortar and then pressed into a pellet to ensure optimal homogeneity and reactivity. The paste was transferred to a 20 mL platinum crucible, which was placed into a muffle furnace heated to 830 °C in the open air for 40 h. In this stage, intermediate grindings were performed every 10 h to improve the completeness of reaction. The purity of the powder pattern was confirmed by powder

XRD studies on a Rigaku DMax-2500/PC powder diffractometer (Rigaku Corporation, Tokyo, Japan) (Figure 1). The syntheses can be expressed by the following equation:

$$3Na_2CO_3 + Sm_2O_3 + 4H_3BO_3 \rightarrow 2Na_3Sm(BO_3)_2 + 3CO_2 + 6H_2O.$$
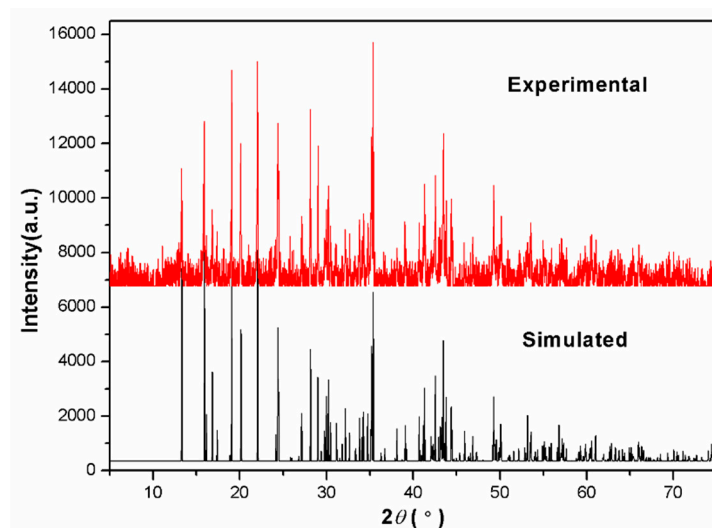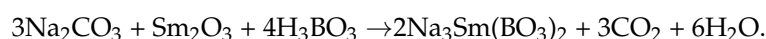
Figure 1. Experimental and simulated X-ray powder diffraction patterns of $Na_3Sm(BO_3)_2$ in the 2θ range of 5–75°.

Single crystal of $Na_3Sm(BO_3)_2$ can be prepared using a high-temperature molten salt method using excess mixture of $Na_2O(Na_2CO_3)$-B_2O_3 as flux, which is the component of the compound $Na_3Sm(BO_3)_2$ to avoid dopant contamination. The mixture of initial reagents Na_2CO_3 (2.000 g, 18.87 mmol), Sm_2O_3 (0.4390 g, 1.258 mmol), and H_3BO_3 (1.944 g, 31.45 mmol), with a molar ratio of 15:1:25, was thoroughly ground in an agate mortar. The mixture was placed in a 20 mL platinum crucible that was heated in a programmable temperature muffle furnace at 900 °C and held at this temperature for 40 h in the open air until the solution became transparent and clear. The homogenized solution was then slowly cooled to 700 °C at a rate of 4 °C·h^{-1} to induce the growth of single crystals. Surprisingly, colorless prism-shaped crystals of $Na_3Sm(BO_3)_2$ were obtained in a yield of about 55% (based on Sm_2O_3), and a high quality crystal with dimensions 0.20 × 0.10 × 0.03 mm was selected for SC-XRD analysis. Some millimeter-sized single crystals with a maximum size of 1.50 × 0.30 × 0.20 mm can be manually selected, washed with hot water, and ground into powder for luminescent property studies.

2.3. Structure Solution

A suitable single crystal with dimensions of 0.20 × 0.10 × 0.03 mm was selected for the single-crystal X-ray diffraction (SC-XRD) experiments. A set of intensity data was collected using a Bruker Smart Apex2 CCD single-crystal diffractometer system equipped with a graphite-monochromated Mo Kα radiation source (λ = 0.71073 Å) with a tube power of 50 kV and 30 mA. The frames were collected at an ambient temperature of 296 K with a scan width of 0.5° in ω and integrated with the Bruker Saint software package using a narrow-frame integration algorithm. The unit cell was determined and refined by the least square method upon the refinement of the *XYZ* centroid of reflections above 20 $\sigma(I)$. No weak satellite reflections were observed and thus no structure modulation was considered in the structure model. Then, the date was scaled for absorption using the SADABS program of Apex2 package [14]. Intensities of all measured reflections were corrected for Lorentz–polarization (Lp) and crystal absorption effects. The crystal structure of $Na_3Sm(BO_3)_2$ was solved by the charge-flipping method using the Superflip program [15] and subsequently refined by the Jana2006 crystallographic computing system [16]. All atoms in the structure were refined using harmonic anisotropic atomic displacement parameters

(ADPs). The details of the data collection and structure refinement are summarized in Table 1, important bond lengths and angles are listed in Table 2, and atomic coordinates and ADPs are given as supporting information (Tables S1 and S2). Further details of the crystal structure investigations can be obtained from the Fachinformationszentrum Karlsruhe, 76344 Eggenstein-Leopoldshafen, Germany (e-mail: crysdata@fiz-karlsruhe.de), on quoting the depository number of CSD-432527.

Table 1. Summary of crystal data and structure refinement of $Na_3Sm(BO_3)_2$.

Chemical Formula	$B_2Na_3O_6Sm$
M_r	336.94
Crystal system, space group	Monoclinic, $P2_1/n$
Temperature (K)	296
a, b, c (Å)	6.5667 (3), 8.7675 (4), 10.1850 (5)
β (°)	90.86
V (Å^3)	586.32 (5)
Z	4
Radiation type	Mo Kα
μ (mm^{-1})	10.20
Crystal size (mm)	$0.20 \times 0.10 \times 0.03$
Diffractometer	Bruker Apex2 CCD
Absorption correction	multi-scan
No. of measured, independent and observed [$I > 2\sigma(I)$] reflections	7164, 1449, 1403
R_{int}	0.025
$(\sin \theta / \lambda)_{max}$ (Å^{-1})	0.666
$R[F^2 > 2\sigma(F^2)]$, $wR(F^2)$, S	0.018, 0.044, 1.14
No. of reflections/ parameters	1449/110
$\Delta\rho_{max}$, $\Delta\rho_{min}$ ($e \cdot$Å^{-3})	1.67, -1.43

Table 2. Selected bond distances (Å) and angles (°) of $Na_3Sm(BO_3)_2$.

Bonds	Distances (Å)	Bonds	Distances (Å)
Sm1—O4	2.338(3)	Na1—O6	2.547(3)
Sm1—O2	2.411(3)	Na1—O5 ^{x}	2.354(3)
Sm1—O5 ^{i}	2.418(2)	Na1—O3 ^{ii}	2.428(3)
Sm1—O1 ^{ii}	2.425(3)	Na1—O1 ^{xi}	2.440(3)
Sm1—O6 ^{iii}	2.471(2)	Na1—O4 ^{iii}	2.497(3)
Sm1—O3 ^{ii}	2.485(2)	Na1—O2 ^{iii}	2.658(3)
Sm1—O6 ^{i}	2.510(2)	Na1—O4	2.573(3)
Sm1—O3	2.518(2)	Na2—O5	2.485(3)
Na3—O1	2.301(3)	Na2—O2 ^{xii}	2.225(3)
Na3—O2	2.375(3)	Na2—O6 ^{viii}	2.467(3)
Na3—O5 ^{vi}	2.350(3)	Na2—O1 ^{ii}	2.666(3)
Na3—O1 ^{vi}	2.893(4)	Na2—O3	2.261(3)
Na3—O5 ^{vii}	3.071(3)	Na2—O4	2.470(3)
B1—O4	1.352(4)	B2—O1	1.372(4)
B1—O5	1.382(4)	B2—O2	1.373(4)
B1—O6	1.399(4)	B2—O3	1.387(4)
Bonds	Angles (°)	Bonds	Angles (°)
O4—B1—O5	121.2(3)	O1—B2—O2	123.2(3)
O4—B1—O6	122.2(3)	O1—B2—O3	117.9(3)
O5—B1—O6	116.5(3)	O2—B2—O3	118.9(3)

Symmetry codes: (i) $x - 1, y, z$; (ii) $-x + 1/2, y + 1/2, -z + 1/2$; (iii) $-x + 1, -y + 2, -z$; (iv) $-x + 1/2, y - 1/2, -z + 1/2$; (v) $x, y - 1, z$; (vi) $-x + 1, -y + 1, -z$; (vii) $x - 1/2, -y + 3/2, z - 1/2$; (viii) $-x + 3/2, y - 1/2, -z + 1/2$; (ix) $x + 1, y, z$; (x) $-x + 3/2, y + 1/2, -z + 1/2$; (xi) $x, y + 1, z$; (xii) $x + 1/2, -y + 3/2, z + 1/2$.

3. Results and Discussion

3.1. Single Crystal Structure

SC-XRD analysis reveals that the compound $Na_3Sm(BO_3)_2$ crystallizes in the Monoclinic system with space group $P2_1/n$. The crystallographic asymmetric unit contains three unique sodium atoms, one unique samarium atom, two unique boron atoms, and six unique oxygen atoms. Each B atom is coordinated by three oxygen atoms into nearly flat BO_3 tetrahedron geometry with three B–O bond lengths of 1.352(4)–1.399(4) Å and bond angles of 116.5(3)–123.2(3)°, which is the common value in borate compounds [17,18]. All BO_3 triangles are isolated in two types of linear array, whereas Na^+ and Sm^{3+} atoms reside among the BO_3 groups and connect them through the columbic action of Na−O and Sm−O to form the structure of $Na_3Sm(BO_3)_2$, as shown in Figure 2. The coordination environments of three Na atoms are different. Na1 atom is coordinated by eight O atoms into $Na1O_8$ polyhedron with Na1−O bond distances ranging from 2.428(3) Å to 2.658(3) Å, whereas Na2 atom connects with six O atoms to form $Na2O_6$ octahedron with Na2−O bond distances ranging from 2.225(3) Å to 2.666(3) Å. The coordination environment Na3 atom is surrounded by five O atoms into a $Na3O_5$ polyhedron with three shorter Na3−O bond distances (2.301(3) Å, 2.350(3) Å, and 2.375(3) Å) and two longer Na3−O bond distances (2.893(4) Å and 3.071(3) Å), which can be considered as secondary coordination bonds to complete the extended coordination spheres of the large Na^+ ion. The coordination mode of $Na3O_5$ shows a big difference from those of $Na1O_7$ and $Na2O_6$, and is an uncommon coordination geometry compared with other reported Na(I) oxide compounds [19]. Although the ionic radii of Sm^{3+} (0.964 Å) is comparable with that of Na^+ (0.950 Å), it adopts a $Sm1O_8$ coordination mode with a Sm1−O bond length of 2.338(3)–2.518(2) Å. In detail, each SmO_8 polyhedron connects with three BO_3 groups via edge-sharing manner, and two BO_3 groups via corner-sharing manner.
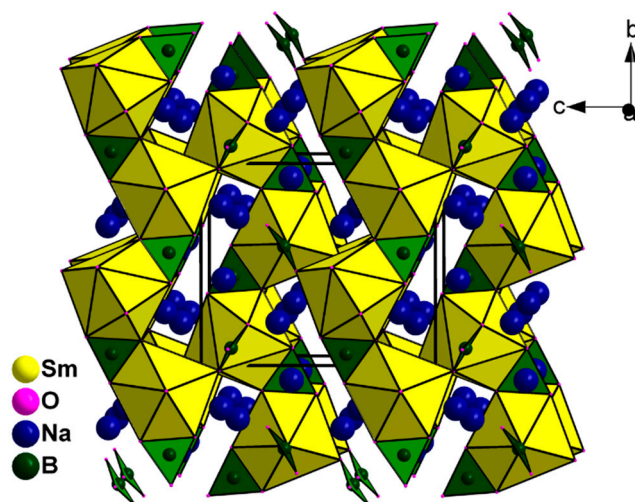
Figure 2. View of the crystal structure of $Na_3Sm(BO_3)_2$ containing BO_3 planes, Na^+ ions, and SmO_8 polyhedra.

The coordination environment of $B1O_3$ and $B2O_3$ groups are shown in Figure 3a,b, respectively. Each $B1O_3$ planar triangle connects to three units ($Na1O_7$, $Na2O_6$, and $Sm1O_8$) via edge-sharing O atoms, and seven units (two $Na1O_7$, one $Na2O_6$, two $Na3O_5$, and two $Sm1O_8$) via corner-sharing O atoms. The coordination environment of the $B2O_3$ unit is similar to that of $B1O_3$ unit; each $B2O_3$ unit coordinates with three units (one $Na3O_5$ and two $Sm1O_8$) via edge-sharing O atoms, and seven units (three $Na1O_7$, three $Na2O_6$ and one $Na3O_5$) via corner-sharing O atoms. Hence, the structure of the compound $Na_3Sm(BO_3)_2$ can be considered a 3D framework that is constructed by NaO_7, NaO_6, NaO_5, SmO_8, and BO_3 units.
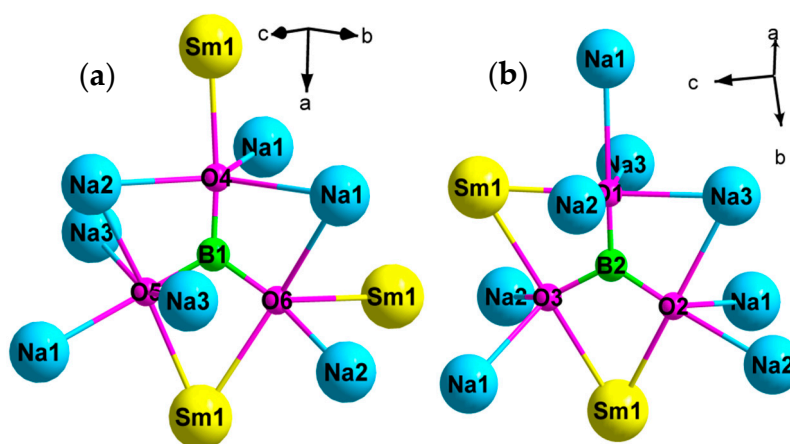
Figure 3. View of the coordination environment of the B1O_3 group (**a**) and the B2O_3 group (**b**).

3.2. Thermal Stability Study

The analysis of TG/DTA illustrates that the compound $Na_3Sm(BO_3)_2$ shows a high stable temperature, as shown in Figure 4. There is no obvious exothermic peak below 900 °C. Upon further heating, $Na_3Sm(BO_3)_2$ started to decompose at 960 °C, and no weight lost was observed until 1000 °C. This result demonstrates a good thermal stability of the compound $Na_3Sm(BO_3)_2$.
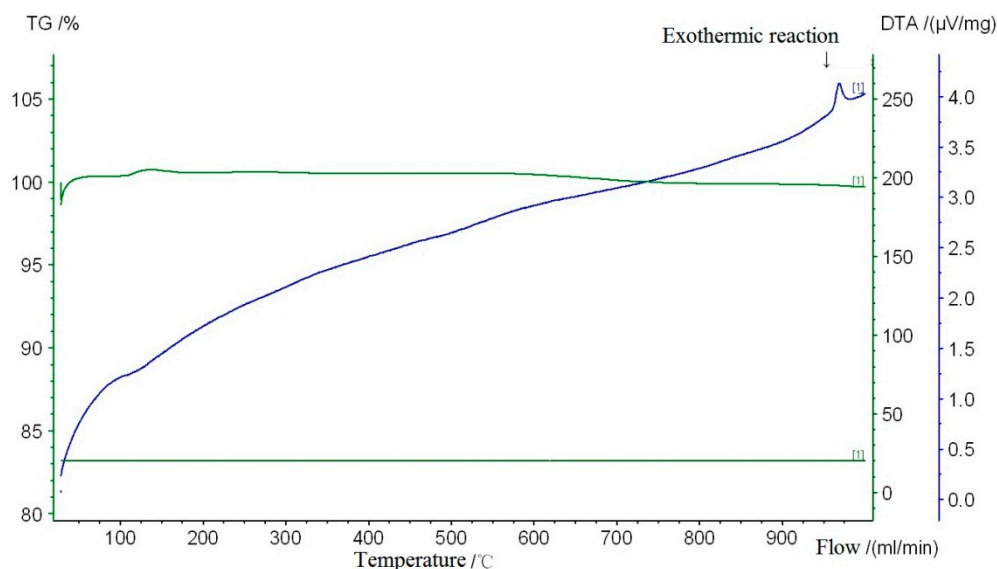
Figure 4. TG and DTA curves for $Na_3Sm(BO_3)_2$.

3.3. UV-Vis Spectroscopic

Figure 5 shows the UV-Vis absorption spectrum of $Na_3Sm(BO_3)_2$ in the range from 240 to 800 nm. The broad absorption band from 240 to 330 nm may correspond to the band-gap transition of $Na_3Sm(BO_3)_2$, whereas the rest sharp absorption from 340 to 500 nm corresponds to typical intra-4f forbidden transitions of the Sm^{3+} ions.
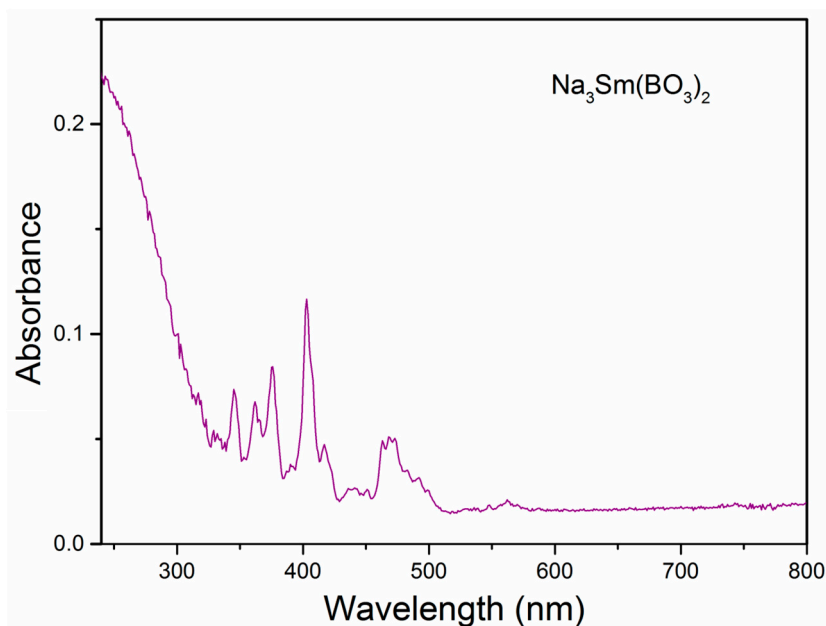
Figure 5. UV-Vis absorption spectrum of the compound $Na_3Sm(BO_3)_2$.

3.4. Luminescent Properties

Although with 100% concentration of Sm^{3+}, the compound $Na_3Sm(BO_3)_2$ exhibits an orange-red emission of Sm^{3+} ion upon excitation with a xenon lamp at near-ultraviolet light. Figure 6a shows the excitation spectrum monitored at the $^4G_{5/2}\rightarrow^6H_{7/2}$ transition of Sm^{3+} with a 605 nm red emission in the range of 350–450 nm. The excitation spectrum consists of a series of peaks centered at 364, 377, 392, 406, 419, and 442 nm, corresponding to the $^6H_{5/2}\rightarrow^4L_{15/2}$, $^6H_{5/2}\rightarrow^6P_{7/2}$, $^6H_{5/2}\rightarrow^4K_{11/2}$, $^6H_{5/2}\rightarrow^4F_{7/2}$, $^6H_{5/2}\rightarrow^4F_{7/2}$, and $^6H_{5/2}\rightarrow(^4G_{9/2}+^4I_{15/2})$ intra-configurational $4f\rightarrow4f$ transition of Sm^{3+} ions, respectively [20,21]. Among these, the $^6H_{5/2}\rightarrow^4F_{7/2}$ transition at 406 nm was the highest intensity, indicating that phosphor $Na_3Sm(BO_3)_2$ can be effectively activated by near-ultraviolet light.

Upon excitation at 406 nm, the emission spectrum is composed of several distinct groups of peaks in the range of 475–750 nm (Figure 6b). There are two strong emissions in the orange-red region coming from positions at 605 nm and 650 nm, corresponding to the $^4G_{5/2}\rightarrow^6H_{7/2}$ and $^4G_{5/2}\rightarrow^6H_{9/2}$ transitions of Sm^{3+}, respectively [22]. Besides, there are two weak emissions centered at 566 nm and 714 nm, which can be assigned to the $^4G_{5/2}\rightarrow^6H_{5/2}$ and $^4G_{5/2}\rightarrow^6H_{11/2}$ transitions of Sm^{3+}, respectively. It is well-known that the emission spectrum of Sm^{3+} activated phosphor strongly depends on the symmetry of the Sm^{3+} site in the host lattice [23,24]. The $^4G_{5/2}\rightarrow^6H_{5/2}$ transition is the magnetic dipole transition, which scarcely changes the crystal field strength around the Sm^{3+} ions, leading to the independence of the symmetry, whereas the transition of $^4G_{5/2}\rightarrow^6H_{9/2}$ is the electric dipole transition, whose intensity is very sensitive to the site symmetry of the Sm^{3+} activators in the host matrix. Although the $^4G_{5/2}\rightarrow^6H_{7/2}$ emission corresponds to the magnetic dipole transition, its magnetic dipole character is usually very low and dominated by the electric dipole (ED) transition. Hence, if the Sm^{3+} occupies the site in a low symmetry, the $^4G_{5/2}\rightarrow^6H_{9/2}$ or $^4G_{5/2}\rightarrow^6H_{7/2}$ emission is frequently the strongest, but in a site with an inversion center, the $^4G_{5/2}\rightarrow^6H_{5/2}$ transition becomes dominant. For $Na_3Sm(BO_3)_2$, it is obviously that the intensity of $^4G_{5/2}\rightarrow^6H_{9/2}$ and $^4G_{5/2}\rightarrow^6H_{7/2}$ emissions is stronger than the $^4G_{5/2}\rightarrow^6H_{5/2}$ emission, which is in good agreement with the crystallographic study that all Sm^{3+} atoms occupy a general site without an inversion center. The quantum efficiency (QE) of a phosphor is an important parameter to be considered for practical applications. The QE can be measured and calculated according to the equation: $\eta_{QE} = \frac{\int L_S}{\int E_R - \int E_S}$, in which the L_S represents the emission spectrum, E_S represents the excitation spectrum, and E_R represents the background. Upon excitation at 406 nm, the corresponding QE of $Na_3Sm(BO_3)_2$ is calculated to be a low value, about 12%.

For the most part, the concentration quenching occurs in 100% Sm^{3+} phosphor $Na_3Sm(BO_3)_2$, and the other affecting factors include preparing temperature, the morphology, and the size of single crystals. Therefore, doping La^{3+} or Gd^{3+} ions into $Na_3Sm(BO_3)_2$ may be an effective method to improve the luminescent QE of $Na_3Sm(BO_3)_2$. This work is still in process.
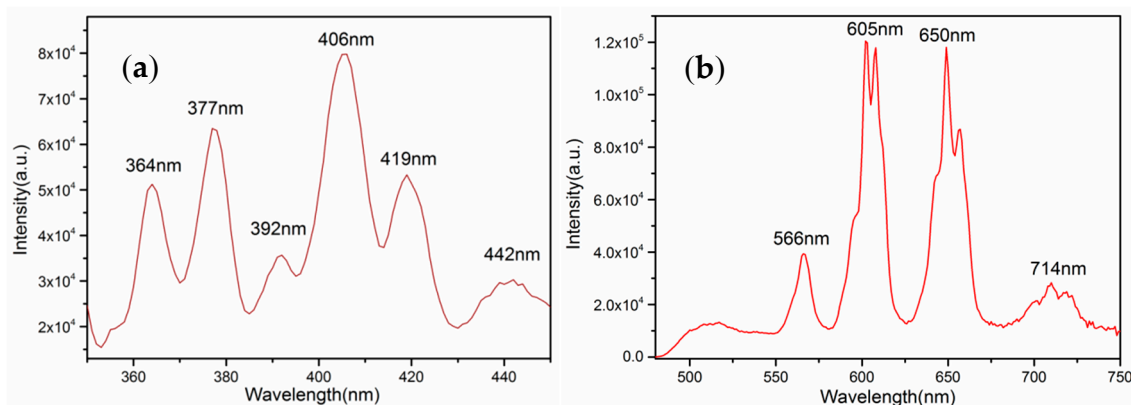
Figure 6. Excitation (**a**) and emission (**b**) spectra of $Na_3Sm(BO_3)_2$.

These three colors are usually referred to as the 1931 color coordinates, the current standard for lighting specifications on the market [25]. In general, the color of any light source in this color space can be represented as an (*x*,*y*) coordinate. The location of the color coordinates of phosphor $Na_3Sm(BO_3)_2$ on the Commission International de l'Éclairage (CIE) chromaticity diagram is presented in Figure 7. Under the excitation at 406 nm, the calculated CIE chromaticity coordinate is (0.660, 0.340), falling in the orange-red region. We may expect that the compound $Na_3Sm(BO_3)_2$ can be used as a good orange-red phosphor.
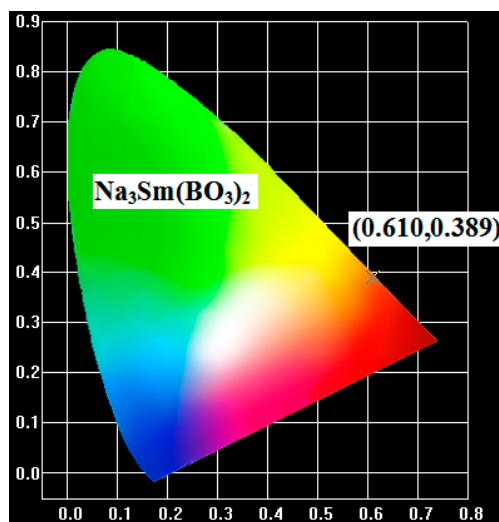
Figure 7. The Commission International de l'Éclairage (CIE) chromaticity diagram for $Na_3Sm(BO_3)_2$ with excitation at 406 nm.

Moreover, we studied the luminescence decay curve for the $^4G_{5/2} \rightarrow ^6H_{7/2}$ emission of Sm^{3+}, as shown in Figure 8. The decay curve cannot be well fitted with a single-exponential but can be well fitted with a bi-exponential function according to the equation [26,27]:

$$I_{(t)} = A_1^* \exp(-t/\tau_1) + A_2^* \exp(-t/\tau_2) + I_{(0)}$$

where $I_{(t)}$ and $I_{(0)}$ are the luminescence intensities at time 0 and t; $A_1{}^*$ and $A_2{}^*$ are the fitting parameters; t is the time; τ_1 and τ_1 are the rapid and slow lifetimes for exponential components, respectively. The double exponential behavior of $Na_3Sm(BO_3)_2$ may originate from energy loss by ion–ion interactions. Then, the average decay time can be calculated to be 1.654 μs to represent the lifetime by the equation [28]:

$$\tau = \frac{A_1\tau_1^2 + A_2\tau_2^2}{A_1\tau_1 + A_2\tau_2}.$$
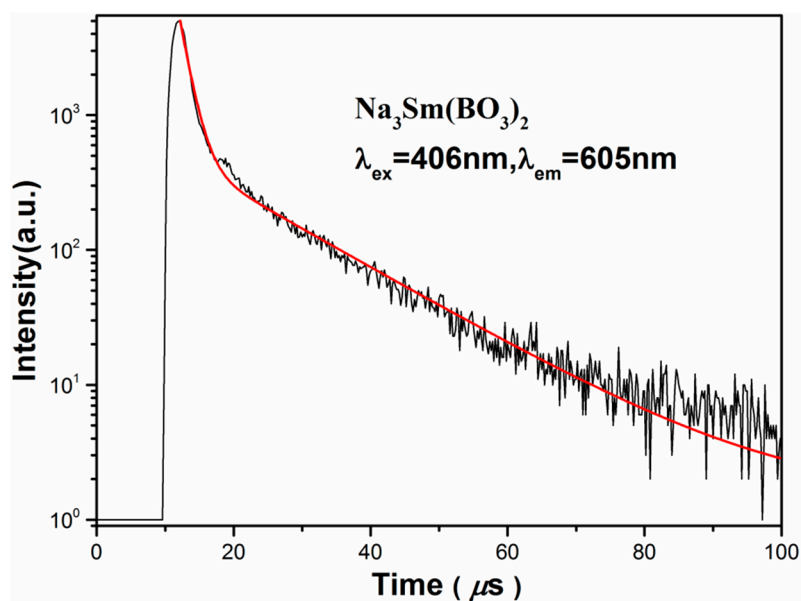
Figure 8. Fluorescent decay (black) and fitting (red) curves of $Na_3Sm(BO_3)_2$.

4. Conclusions

A new type of sodium samarium borate $Na_3Sm(BO_3)_2$ was prepared using a high temperature molten salt (flux) method and its structure was determined by SC-XRD analyses. Compound $Na_3Sm(BO_3)_2$ crystallizes in the monoclinic *P*-centered space group $P2_1/n$. The structure of the compound $Na_3Sm(BO_3)_2$ can be considered as a 3D framework that is constructed by NaO_7, NaO_6, NaO_5, SmO_8, and BO_3 units. Even with the 100% Sm^{3+} ion concentration, $Na_3Sm(BO_3)_2$ shows intense luminescent emission behavior. The excitation spectra cover a wide range from 350 to 450 nm, which suggests that the phosphor $Na_3Sm(BO_3)_2$ can be effectively excited by a near-UV light source. The emission spectrum excited at 406 nm shows two strong emission bands in the orange-red region: 605 nm ($^4G_{5/2} \rightarrow {}^6H_{9/2}$) and 650 nm ($^4G_{5/2} \rightarrow {}^6H_{7/2}$). The CIE chromaticity color coordinates ($x = 0.660$, $y = 0.340$) were found to be in the orange-red region of the chromaticity diagram. The decay curve excited by 406 nm was measured and the decay time was fitted to be 1.654 μs. We think $Na_3Sm(BO_3)_2$ can be potentially used as an orange-red phosphor under near-UV light excitation.

Author Contributions: Dan Zhao conceived and designed the experiments, and wrote the paper; Fa-Xue Ma, Cong-Kui Nie and Lei Zhang performed the experiments; Jian Wang analyzed the data; Yunchang Fan contributed reagents/materials/analysis tools.

Conflicts of Interest: The authors declare no conflict of interest.

References

1. Kim, K.Y.; Yoon, S.J.; Park, K. Synthesis and photoluminescence properties of red-emitting $Ca_{3-3x/2}(VO_4)_2$:XEu^{3+} phosphors. *J. Lumin.* **2015**, *160*, 78–84. [CrossRef]

2. Zhao, D.; Ma, F.-X.; Zhang, R.-J.; Li, F.-F.; Zhang, L.; Yang, J.; Fan, Y.-C.; Xin, X. Structure modulation, band structure, density of states and luminescent properties of columbite-type $ZnNb_2O_6$. *Crystengcomm* **2016**, *18*, 2929–2936. [CrossRef]

3. Barsukova, M.; Goncharova, T.; Samsonenko, D.; Dybtsev, D.; Potapov, A. Synthesis, crystal structure, and luminescent properties of new zinc(ii) and cadmium(ii) metal-organic frameworks based on flexible bis(imidazol-1-yl) alkane ligands. *Crystals* **2016**, *6*, 132. [CrossRef]

4. Li, H.L.; Liu, Y.J.; Zheng, R.; Chen, L.J.; Zhao, J.W.; Yang, G.Y. Trigonal pyramidal {$AsO_2(OH)$} bridging tetranuclear rare-earth encapsulated polyoxotungstate aggregates. *Inorg. Chem.* **2016**, *55*, 3881–3893. [CrossRef] [PubMed]

5. Zhang, W.-L.; Lin, C.-S.; He, Z.-Z.; Zhang, H.; Luo, Z.-Z.; Cheng, W.-D. Syntheses of three members of $A^{(ii)}M^{(iv)}(PO_4)_2$: Luminescence properties of $PbGe(PO_4)_2$ and its Eu^{3+}-doped powders. *Crystengcomm* **2013**, *15*, 7089–7094. [CrossRef]

6. Kalidasan, M.; Asokan, K.; Dhanasekaran, R. Luminescence properties of 100 mev W^{8+} ion irradiated $GdCa_4O(BO_3)_3$:Eu^{3+} and $GdCa_4O(BO_3)_3$:Tb^{3+} phosphors. *J. Lumin.* **2016**, *180*, 241–250. [CrossRef]

7. Yang, L.; Wan, Y.; Huang, Y.; Chen, C.; Seo, H.J. Development of $YK_3B_6O_{12}$:Re (Re = Eu^{3+}, Tb^{3+}, Ce^{3+}) tricolor phosphors under near-uv light excitation. *J. Alloys Compd.* **2016**, *684*, 40–46. [CrossRef]

8. Mascetti, J.; Vlasse, M.; Fouassier, C. The Crystal Chemistry of the New Rare-Earth Sodium Borates $Na_3Ln(BO_3)_2$(Ln = La, Nd). *J. Solid State Chem.* **1981**, *39*, 288–293. [CrossRef]

9. Wang, Z.X.; Li, H.K.; Cai, G.M.; Jin, Z.P. Synthesis, crystal structure, and thermal stability of new borates $Na_3REB_2O_6$(RE = Pr, Sm, Eu). *Powder Diff.* **2016**, *31*, 110–117. [CrossRef]

10. Wang, S.; Ye, N.; Poeppelmeier, K.R. Flux growth and crystal structure refinement of calcite type borate $GaBO_3$. *Crystals* **2015**, *5*, 252–260. [CrossRef]

11. Yu, N.; Wang, S.; Ye, N.; Liang, F.; Lin, Z.; Luo, M.; Poeppelmeier, K.R. A deep-ultraviolet nonlinear optical crystal: Strontium beryllium borate fluoride with planar Be(O/F)$_3$ groups. *Chem. Mater.* **2016**, *28*, 4563–4571. [CrossRef]

12. Abudoureheman, M.; Han, S.; Lei, B.-H.; Yang, Z.; Long, X.; Pan, S. $KPb_2(PO_3)_5$: A novel nonlinear optical lead polyphosphate with a short deep-UV cutoff edge. *J. Mater. Chem. C* **2016**, *4*, 10630–10637. [CrossRef]

13. Zhen, N.; Nian, L.; Li, G.; Wu, K.; Pan, S. A high laser damage threshold and a good second-harmonic generation response in a new infrared NLO material: $LiSm_3SiS_7$. *Crystals* **2016**, *6*, 121. [CrossRef]

14. *Bruker, APEX2 and SAINT*; Version 2013.11-0; Bruker AXS Inc.: Madison, WI, USA, 2013.

15. Palatinus, L.; Chapuis, G. Superflip—A computer program for the solution of crystal structures by charge flipping in arbitrary dimensions. *J. Appl. Crystallogr.* **2007**, *40*, 786–790. [CrossRef]

16. Petricek, V.; Dusek, M.; Palatinus, L. Crystallographic computing system Jana2006: General features. *Z. Kristallogr.* **2014**, *229*, 345–352.

17. Yu, H.; Young, J.; Wu, H.; Zhang, W.; Rondinelli, J.M.; Halasyamani, P.S. Electronic, crystal chemistry, and nonlinear optical property relationships in the dugganite $A_3B_3Cd_2O_{14}$ family. *J. Am. Chem. Soc.* **2016**, *138*, 4984–4989. [CrossRef] [PubMed]

18. Zhang, W.; Yu, H.; Wu, H.; Halasyamani, P.S. Crystal growth and associated properties of a nonlinear optical crystal-$Ba_2Zn(BO_3)_2$. *Crystals* **2016**, *6*, 68. [CrossRef]

19. Zhao, D. Heptasodium tetraaluminium tetrakis (diphosphate) orthophosphate, $Na_7Al_4(P_2O_7)_4(PO_4)$. *Acta Crystallogr. Sect.* **2011**, *67*, I64. [CrossRef] [PubMed]

20. Vishwakarma, A.K.; Jayasimhadri, M. Pure orange color emitting Sm^{3+} doped $BaNb_2O_6$ phosphor for solid-state lighting applications. *J. Lumin.* **2016**, *176*, 112–117. [CrossRef]

21. Sun, J.F.; Ding, D.B.; Sun, J.Y. Synthesis and photoluminescence properties of a novel reddish orange-emitting Sm^{3+}-doped strontium borosilicate phosphor. *Opt. Mater.* **2016**, *58*, 188–195. [CrossRef]

22. Yawalkar, M.M.; Zade, G.D.; Dabre, K.V.; Dhoble, S.J. Luminescence study of Eu^{3+}-doped $Li_6Y(BO_3)_3$ phosphor for solid-state lighting. *Luminescence* **2016**, *31*, 1037–1042. [CrossRef] [PubMed]

23. Zhou, R.; Wang, L.X.; Xu, M.J.; Jia, D.Z. Photoluminescence characteristics of Sm3+ doped $Sr_2P_2O_7$ as new orange-red emitting phosphor. *J. Alloys Compd.* **2015**, *647*, 136–140. [CrossRef]

24. Yang, Z.; Xu, D.; Sun, J.; Sun, Y.; Du, H. Characterization and luminescence properties of $Sr_3Gd(PO_4)_3$: Sm^{3+} orange-red phosphor. *Opt. Eng.* **2015**, *54*, 105102. [CrossRef]

25. Shionoya, S.; Yen, W.M. *Phosphor Handbook*; Phosphor Research Society, CRC Press: Boca Raton, FL, USA, 1998; pp. 459–465.

26. Zeng, C.; Huang, H.W.; Hu, Y.M.; Miao, S.H.; Zhou, J. A novel blue-greenish emitting phosphor $Ba_3LaK(PO_4)_3F$:Tb^{3+} with high thermal stability. *Mater. Res. Bull.* **2016**, *76*, 62–66.

27. Zhang, D.J.; Wang, X.M.; Qiao, Z.A.; Tang, D.H.; Liu, Y.L.; Huo, Q.S. Synthesis and Characterization of Novel Lanthanide(III) Complexes-Functionalized Mesoporous Silica Nanoparticles as Fluorescent Nanomaterials. *J. Phys. Chem. C* **2010**, *114*, 12505–12510. [CrossRef]

28. Annadurai, G.; Kennedy, S.M.M. Synthesis and photoluminescence properties of $Ba_2CaZn_2Si_6O_{17}$:Eu^{3+} red phosphors for white LED applications. *J. Lumin.* **2016**, *169*, 690–694. [CrossRef]